Human contribution to the record-breaking July 2019 heat wave in Western Europe

Robert Vautard, Olivier Boucher (IPSL Paris)
Geert Jan van Oldenborgh (KNMI)
Friederike Otto, Karsten Haustein (University of Oxford)
Martha M. Vogel, Sonia I. Seneviratne (ETH Zürich)
Jean-Michel Soubeyroux, Michel Schneider, Agathe Drouin, Aurélien Ribes (Météo France)
Frank Kreienkamp (Deutscher Wetterdienst)
Peter Stott (UK Met Office)
Maarten van Aalst (ITC/University of Twente and Red Cross Red Crescent Climate Centre)

Key findings

- **A second record-breaking heat wave of 3-4 days took place in Western Europe in the last week of July 2019, with temperatures exceeding 40 degrees in many countries including Belgium and the Netherlands where temperatures above 40°C were recorded for the first time. In the U.K. the event was shorter lived (1-2 days), yet a new historical daily maximum temperature was recorded exceeding the previous record set during the hazardous August 2003 heatwave.**

- **In contrast to other heat waves that have been attributed in Western Europe before, this July heat was also a rare event in today's climate in France and the Netherlands. There, the observed temperatures, averaged over 3 days, were estimated to have a 50-year to 150-year return period in the current climate. Note that return periods of temperatures vary between different measures and locations, and are therefore highly uncertain.**

- **Combining information from models and observations, we find that such heatwaves in France and the Netherlands would have had return periods that are about a hundred times higher (at least 10 times) without climate change. Over France and the Netherlands, such temperatures would have had extremely little chance to occur without human influence on climate (return periods higher than ~1000 years).**

- **In the U.K. and Germany, the event is less rare (estimated return periods around 10-30 years in the current climate) and the likelihood is about 10 times higher (at least 3 times) due to climate change. Such an event would have had return periods of from a few tens to a few hundreds of years without climate change.**

- **In all locations an event like the observed would have been 1.5 to 3 ºC cooler in an unchanged climate.**

- **As for the June heatwave, we found that climate models have systematic biases in representing heat waves at these time scales and they show about 50% smaller trends than observations in this part of Europe and much higher year-to-year variability than the observations. Despite this, models still simulate very large probability changes.**

- **Heatwaves during the height of summer pose a substantial risk to human health and are potentially lethal. This risk is aggravated by climate change, but also by other factors such as an aging population, urbanisation, changing social structures, and levels of preparedness. The full impact is only known after a few weeks when the mortality figures have been analysed. Effective heat emergency plans, together with accurate weather forecasts such as those issued before this heatwave, reduce impacts and are becoming even more important in light of the rising risks.**

- **It is noteworthy that every heatwave analysed so far in Europe in recent years (2003, 2010, 2015, 2017, 2018, June 2019 and this study) was found to be made much more likely and more intense due to human-induced climate change. How much more depends very strongly on the event definition: location, season, intensity and durations. The July 2019 heatwave was so extreme over continental Western Europe that the observed magnitudes would have been extremely unlikely without climate change.**

Introduction, Trigger

After the extreme heat that took place in the last week of June 2019, a second record-breaking heatwave struck Western Europe and Scandinavia at the end of July 2019. In June, new all-time records were set in multiple places across Western Europe. In July, records were broken again, albeit in different areas. Taking into account both episodes, the spatial extent of broken historical records is large: in most areas of France, the Benelux, Switzerland, in western Germany, Eastern U.K. and Northern Italy. Some of these previous records were set as early as the 1950s, with some stations setting new records that have continuously been monitoring the weather for more than 200 years (e.g. Oxford, UK). Figure 1 shows the areas of Europe were records were set. A detailed overview on the meteorological conditions of July heatwave and its development and impacts on e.g. Greenland ice melting can be found in the report of the World Meteorological Organization (WMO) under https://public.wmo.int/en/media/news/july-heatwave-has-multiple-impacts .

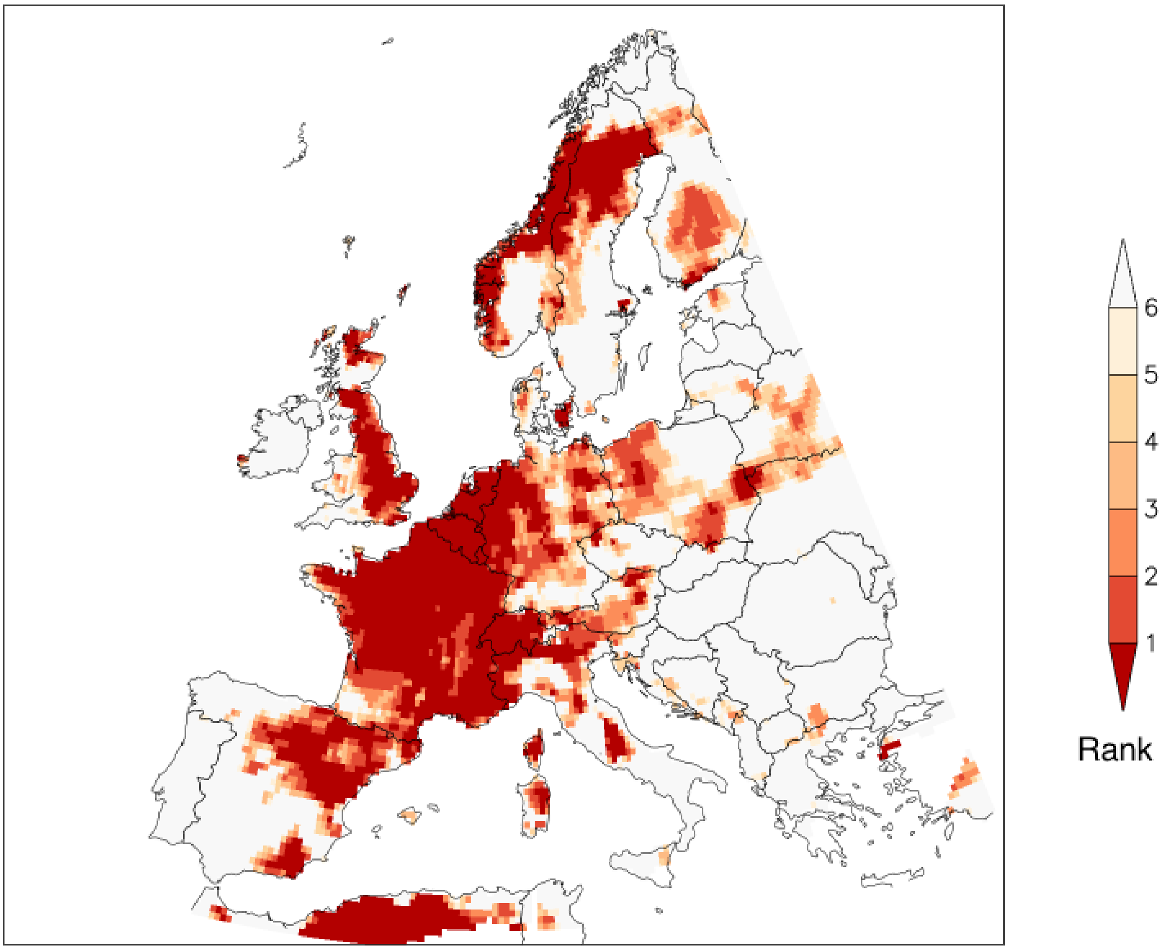

Figure 1: Rank of annual maximum temperatures observed in Europe in 2019 compared to 1950 - 2018, based on the E-OBS data set (Haylock et al., 2008, version 19, extended with monthly and daily updates to 30 July 2019). This figure is made with preliminary data and should be taken with caution as some measurements are not yet validated.

The July episode was rather short and intense, with about four days of very high temperatures. In France, the highest amplitudes of the heatwave were found in Northern and Central parts of the country, with records of either 1947 or 2003 broken by a large departure on 25 July. For instance, the historical record of Paris (Station Paris-Montsouris) of 40.4°C became 42.6°C and a temperature of 43.6°C was measured in Saint Maur des Fossés a few kilometers away from Paris city in a residential area. In Belgium and the Netherlands for the first time ever temperatures above 40°C were observed. In Germany the historical record of 40.3 °C (in Kitzingen, 2015) has been surpassed by almost 1°C (41.2°C at two stations) on 25 July, with one station reaching 42.6 °C (Lingen), which is thus the new - officially confirmed - German temperature record. In total, the old record was exceeded at 15 stations in Germany. In the UK, a new highest ever maximum temperature of 38.7°C was measured in Cambridge. Further west, where the heatwave was slightly less intense, the record from 1932 (35.1°C) at the historic Oxford Radcliffe Meteorological Station (continuous measurements for more than 200 years) was broken by more than one degree, with the new record maximum temperature of 36.5°C.

While the new records made headlines, such extreme temperatures are dangerous, in particular when prolonged over several days and nights. Heatwaves are known to increase mortality, especially among those with existing respiratory illnesses and cardio-vascular disease, despite the fact that the quantification of heat-related fatalities is not straightforward to assess and thus not known in near-real time. However, compared to the 2003 heatwave, this time authorities were better prepared. Heatwave action plans, aiming at preventing a catastrophic scenario such as in 2003, when more than 15,000 people died in France alone, are now in place. Preparedness was also facilitated by very accurate weather forecasts from the national met services. Several European weather services have issued heat warnings. For instance, the temperatures of 42-43°C in Paris were consistently forecast 3-4 days ahead by Météo-France.

In a relatively similar way to the June case, the July heat wave occurred due to a ridge across western Europe (highly amplified Rossby wave), together with a low-pressure system developing offshore the Iberian peninsula, as shown in Figure 2. This weather pattern induced intense advection of hot air from North Western Africa across Spain to France (Figure 3) and then Germany and the Benelux, eventually reaching Scandinavia a few days later. In contrast to the June heatwave, this July heatwave was accompanied by severe drought conditions in areas such as France (a majority of French territory was under drought regulation measures), which might have been a confounding factor given that dry soils are suspected to cause an additional temperature increase at regional scales due to land-atmosphere feedbacks (Seneviratne et al., 2010). Other regions were also shown to be affected by drier conditions, in particular in Germany and Central Europe (e.g. ASCAT satellite measurements).

In the following we will present the results of an attribution analysis following the same methodology used in the previous analysis on the June heatwave (https://www.worldweatherattribution.org/human-contribution-to-record-breaking-june-2019-heatwave-in-france/), and as introduced in several earlier peer-reviewed assessments (e.g., Kew et al, 2018, Philip et al, 2018, Otto et al., 2017). We refer to these studies for a detailed explanation of methods and models.

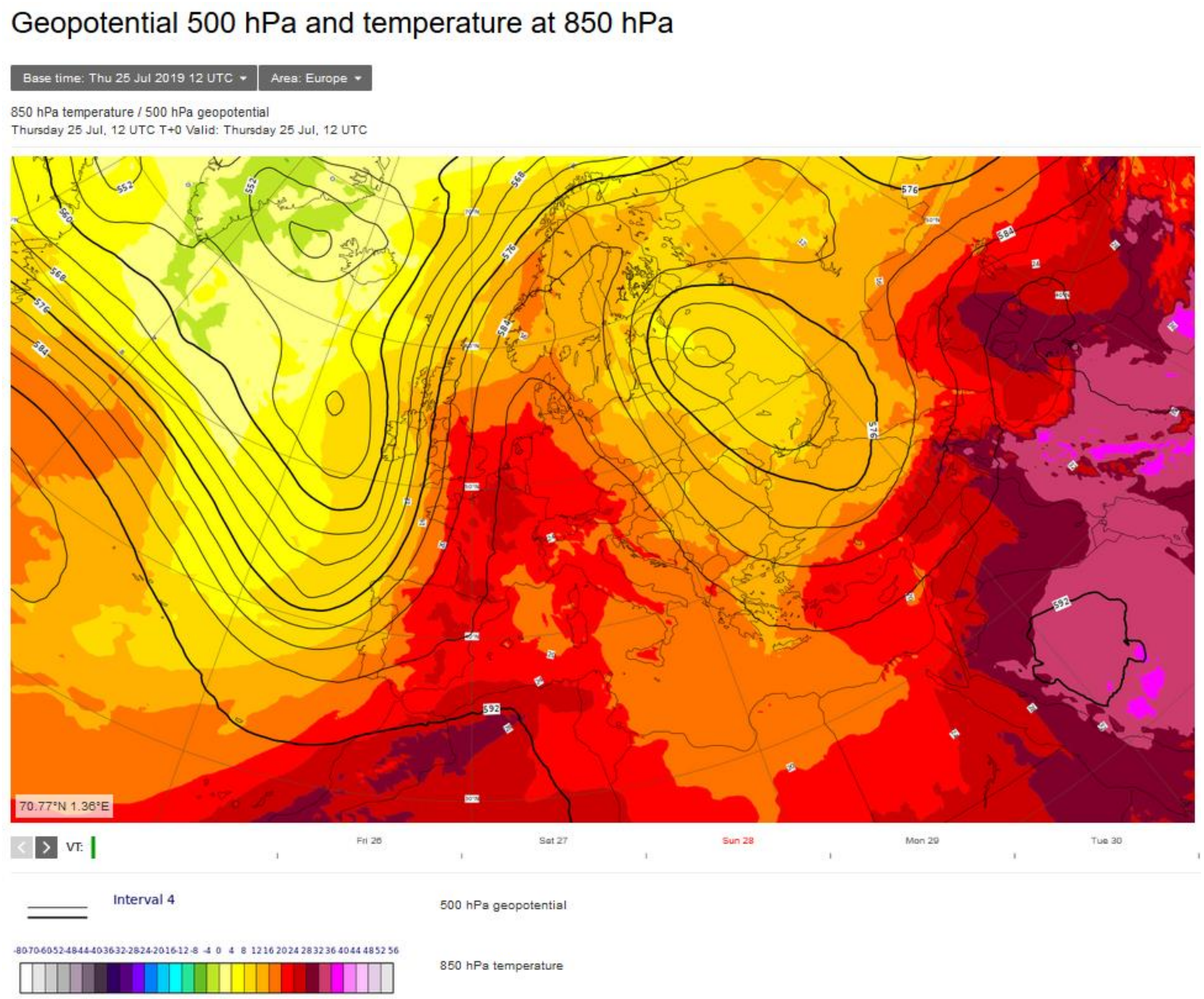

Figure 2: Temperature field of the 25 July 2019 12 UTC at 850 hPa (colors) together with 500 hPa (isolines) as obtained from ECMWF analyses (figure taken from the forecast website: (https://www.ecmwf.int/en/forecasts/charts/catalogue/medium-z500-t850-public?facets=Range,Medium%20(15%20days)&time=2019072512,0,2019072512&projection=classical_europe).

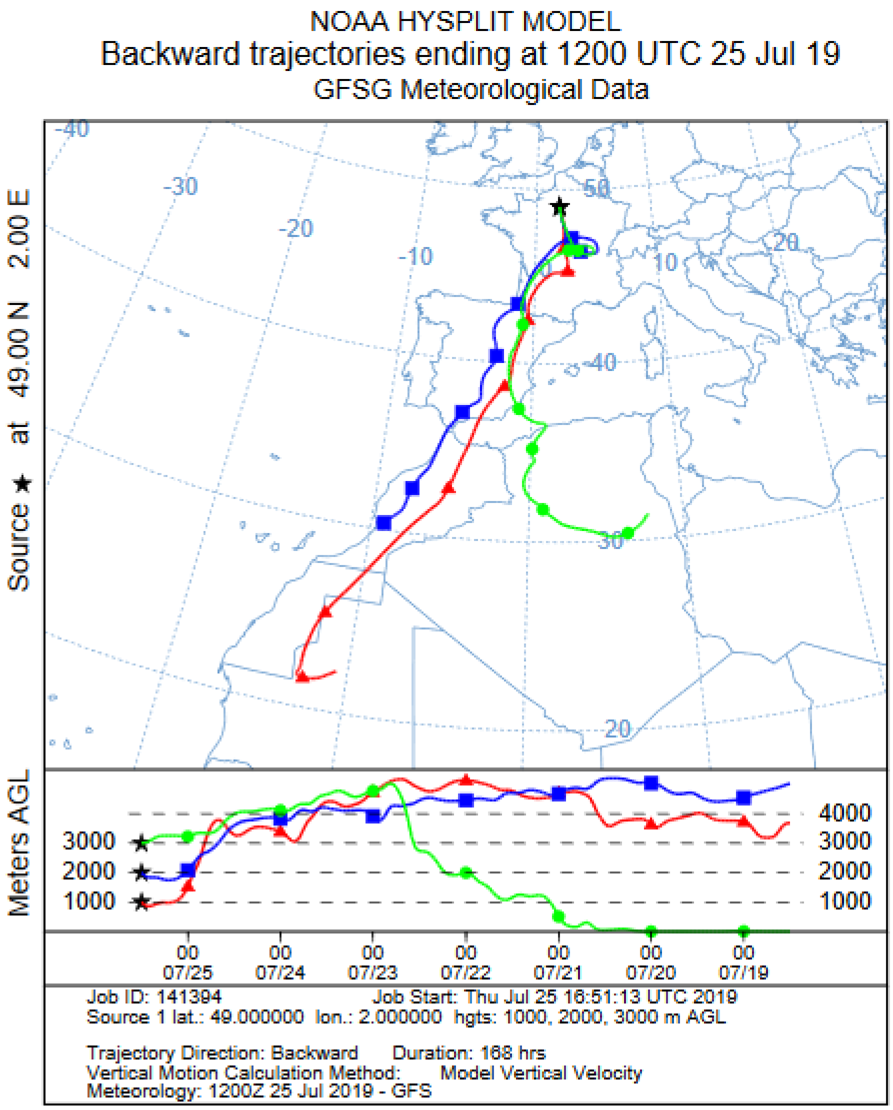

Figure 3: 7-day Back-trajectories ending near Paris at 1000, 2000 and 3000 m as obtained from NCEP analyses and the HySplit trajectory model from NOAH.

Event definition

As in June, we use an event definition that represents the impacts on humans, by combining both daytime and nighttime heat and also the persistence of the episode beyond a few days. We defined the event as the highest 3-day averaged daily mean temperature for each year (TG3x). The time span of the indicator almost corresponds or exceeds the length of the heat wave period. This may be one reason why the indicator has lower values at some stations than during the heat wave in 2003.

Thus in this study we are aiming to answer the question whether and how the probability of 3-day average temperature as high or higher than the observed temperature in different places in Western Europe has changed as a result of human-induced climate change. A map of the rank of TG3x in 2019 is very similar to Fig.1 (not shown).

In order to give a flavour of how this heatwave was felt in different places in Europe, we selected several locations in France, Germany, The Netherlands and the U.K.; countries in which a number of temperature records were broken, and data were readily availability through study participants or public websites.

The locations considered are shown in Table 1. The average over metropolitan France is close to the value of the official French thermal index (used in the June heatwave study), which averages temperature over 30 sites well distributed over the metropolitan area and is used to characterize heat waves and cold spells at the scale of the country. The rest of the analysis is based on a set of 5 individual weather stations. We selected the stations based on the availability of data, their series length (at least starting in 1951) and avoidance of urban heat island (UHI) and Irrigation Cooling Effects (ICE), which result in non-climatic trends. The locations considered all witnessed a historical record both in daily maximum and in 3-day mean temperature (apart from Oxford and Weilerswist-Lommersum where only daily maximum temperatures set a record). Further, the selected stations are either the nearest station with a long enough record to where the study authors reside, or representing a national record. During the analysis we also gained access to the unreleased homogenised daily time series from Uccle (Brussels). The trend in observations is very similar to Lille and De Bilt, but we could not include it fully in the analysis.

Table 1: the locations considered for the event definition

Location	Observation source	Longitude	Latitude	Data start
France metropolitan Average	E-OBS Thermal index			1950 1947
Lille Lesquin (FR)	ECA&D	3.15°E	50.97°N	1945
De Bilt (NL)	KNMI	5.18°E	52.10°N	1901
Cambridge BG (UK)	MOHC	0.13°E	52.19°N	1911
Oxford (UK)	Univ Oxford	-1.27°E	51.77°N	1815
Weilerswist-Lommersum (DE)	DWD	6.79°E	50.71°N	1937

The De Bilt station has been statistically corrected for a change in hut from a pagoda to a Stevenson screen in 1950 and a move from a sheltered garden to an open field in 1951.

The Cambridge Botanical Gardens (BG) station that observed the UK record temperature of 38.7 ºC has a sizeable fraction of missing data. On 23 July there were battery issues, this value has been estimated by the UK Met Office on the basis of their interpolation routine. For earlier years we used the values of the nearby Cambridge NIAB station with a linear bias regression T(BG) = (1+A) T(NIAB) + B, with A about 5% in summer and B -0.6 ºC in July, -0.9 ºC in August.

The German temperature was highest in Lingen, but there were debates about the validity of the measured value. While it is now officially confirmed by the Deutscher Wetterdienst (DWD), here we opted to analyse the nearby station Weilerswist-Lommersum. This rural station has observations going back to 1937 with two years missing (December 1945 to November 1946 and September 2003 to July 2004). Yet the two hot summers of 1947 (TG3x 0.8 ºC cooler than 2019) and 2003 (TG3x 0.1 ºC hotter) are included.

Trend in observations

There is a clear trend in observed annual values of the event indicators in each case (see Figure 4), and the 2019 value represents a large excursion away from the average. This is in particular the case for continental stations where the heatwave lasted longer.

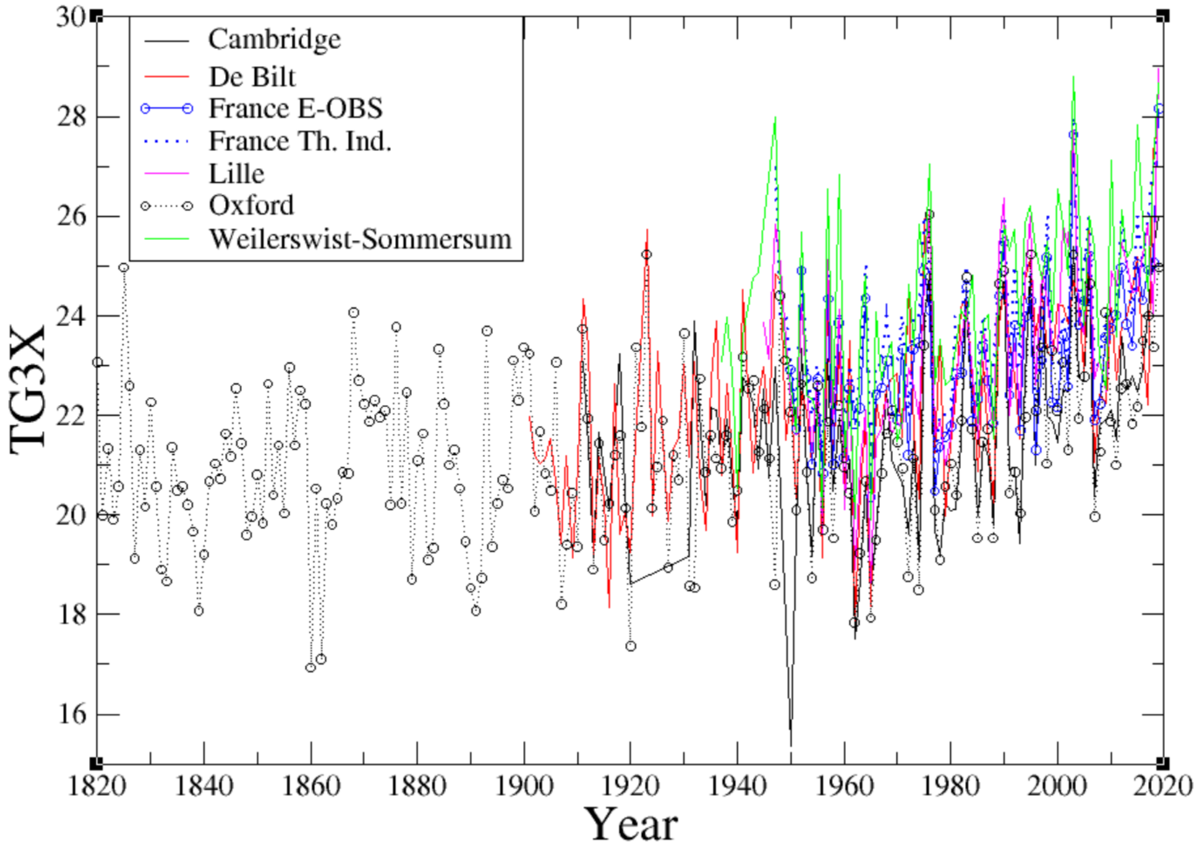

Figure 4: Time series of the temperature index at locations considered (°C).

The trend in observed series is quantified using the properties of the fit of a Generalized Extreme Value (GEV) analysis with a covariate (smoothed Global Mean Surface Temperature, GMST) representing an indicator of climate change (from anthropogenic and natural factors) on the position parameter, keeping the scale and shape parameters constant. Comparison with climate models (where individual drivers of change can be isolated) show that this assumption is justified. It should be noted that for extreme heat the GEV has a negative shape parameter, which describes an upper bound to the distribution. This bound is however increased by global warming. If the temperature in 2019 is above the bound in 1900, the probability of the event occurring without the warming trend is zero and the probability ratio formally infinite, subject to the assumptions made.

The change in intensity for similarly likely heat waves varies between 2°C and 3.5°C depending on the location. The return periods range from about 8 years in Oxford to 80 years in Lille. For the Metropolitan France average, best estimates of the return periods are of the order of 130 years (the spatial averaging emphasises the trend over the weather noise). In France, Benelux and Germany the return periods for stations are relatively similar (60-80 years). In Germany for the selected station we find a return period of 12 years. This relatively low return period could be due to the fact that the station is located on the eastern edge of the affected region. Note that we found much higher return periods at the record station Lingen. However, given an initial controversy surrounding the validity of this station, it was discarded for our analysis. In the U.K., return periods are shorter because the event was in fact shorter than 3 days and 3-day averages there mix hot temperatures with cooler ones. As seen in Table 2, uncertainties on the return period are very large which leads to similarly large uncertainties for the Probability Ratios with many cases where an upper bound is infinite. In a few cases the best fit also gives zero probability in 1900 thus only a lower bound can be given.

Table 2: Statistical quantities linked to the trend in the observed values of the indicator.

Location	Value 2019 (°C)	Return Period 2019 (Yr)	Probability Ratio	Change in intensity (°C)
France Avg.	E-OBS: **28.2** Météo-Fr: **28.7**	**134** *[>30]*	**>5**	**2.5** *[1.5 - 3.4]*
Lille Lesquin	**29.1**	**78** *[>20]*	**>20**	**3.5** *[2.3 - 4.6]*
De Bilt	**28.0**	**60** *[20 - 1400]*	**>60**	**2.9** *[2.0 - 3.7]*
Cambridge BG	**26.0**	**28** [11 - 200]	**250** [9 - ∞]	**2.3** [1.4 - 3.4]
Oxford	**25.0**	**7.7** *[4.6 - 16]*	**12** *[5 - 290]*	**2.1** *[1.3 - 2.9]*
Weilerswist-Lommersum	**28.7**	**12** *[6 - 60]*	**430 [18 -** ∞]	**3.4** *[2.2 - 4.9]*

Model evaluation

For the attribution analysis we used a set of 8 climate model ensembles including the multi-model ensembles EURO-CORDEX and CMIP5, and single-model ensembles from the CMIP5 and CORDEX generation (EC-EARTH, RACMO, weather@home) as well as two models from the CMIP6 generation (IPSL-CM6-LR and CNRM-CM6.1). Table 3 summarizes the characteristics of the model ensembles. The Appendix provides more details.

Table 3: Overview of models used in this study

Name	Description	Period	Resolution (atmospheric GCM or RCM)
EURO-CORDEX	10 ensemble members of different RCM/GCM combinations, bias-corrected at IPSL. historical/RCP4.5.	1971-2019	12.5 km
CMIP5	28 simulations from different global climate models which contributed to the 5th phase of the Coupled Modeling Intercomparison Project (CMIP5), bias-corrected	Historical: 1870-2005 RCP8.5: 2005-2100	Between 0.5°x 0.5° to 4°x 4° (between ~50 km and ~400 km)

	against E-OBS at ETHZ.		
weather@home	large ensemble of HadRM3P embedded in HadAM3P with prescribed SST, counterfactual 11 different SST patterns subtracted	2006-2015 vs counterfactual 2006-2015	25 km
RACMO 2.2	16 ensemble members downscaling EC-Earth 2.3 historical/RCP8.5 runs	1950-2019	11 km
HadGEM3-A trend	EUCLEIA 15-member ensemble, SST-forced.	1961-2015	N216 (~60 km)
EC-Earth 2.3	16-member ensemble coupled GCM, historical/RCP8.5	1861-2019	T159 (~150 km)
IPSL-CM6A-LR	31-member ensemble coupled GCM, CMIP6 historical (1850-2014) prolonged until 2029 with SSP585 forcing except for constant 2014 tropospheric aerosol forcings	1850-2029	144x142 grid points (~160 km on average)
CNRM-CM6.1	10-member ensemble coupled GCM, CMIP6 historical	1850-2014	1.4° at the equator, with 91 vertical layers

Figure 5 compares the GEV distribution parameters between model ensembles and observations. In general, the same conclusions hold regarding models skill as in our analysis of the June heatwave. Models have a too high variability and hence overestimate the sigma parameter, sometimes by a large amount (factor 1.5 to 2.5). This is particularly marked for the France average. However, HadGEM3-A, EC-EARTH, IPSL-CM6-LR and CNRM-CM6.1 appear to have a reasonable departure from observations. For the other models the 95% confidence intervals on the scale parameter does not overlap with the confidence interval on the scale parameter from the observations, which is our criterion for inclusion of the models in the attribution.

For individual stations studied here shape parameters are well simulated. The discrepancy for the scale parameter is also reduced except for weather@home where variability remains too high. The difference in behavior between the France average and the stations could arise from several reasons and remains to be investigated. Averaging itself is probably not the reason as the large discrepancy was also found in June for the Toulouse site. The issue requires an in-depth investigation, but probable reasons may be in a difficulty of models to correctly simulate land-atmosphere interactions, resulting in a deficit of skill for the simulation of heatwaves especially in regions where evapotranspiration regimes undergo transitions from energy-limited to soil-moisture limited regimes. Preliminary investigations into the deficits of weather@home have shown that an insufficient cloud cover in the model leads to unrealistically high hot extremes and low cold extremes. Another possible cause is dynamical as France may occasionally be influenced by episodic advection of hot and dry air from Spain and North Africa leading to large excursions of temperature which models might not capture well.

In Lille, weather@home and HadGEM3-A fail the test that the scale parameter is compatible with the observed range.

At Weilerswist-Lommersum and De Bilt, all models except weather@home pass our model evaluation criterion of the observed parameter uncertainty range overlapping the modelled ones.

In Cambridge and Oxford, the CMIP5 ensemble, IPSL-CM6A-LR and CNRM-CM6.1 have a too large scale parameter σ compared to the observations, weather@home much too large. We therefore do not include these models in the attribution.

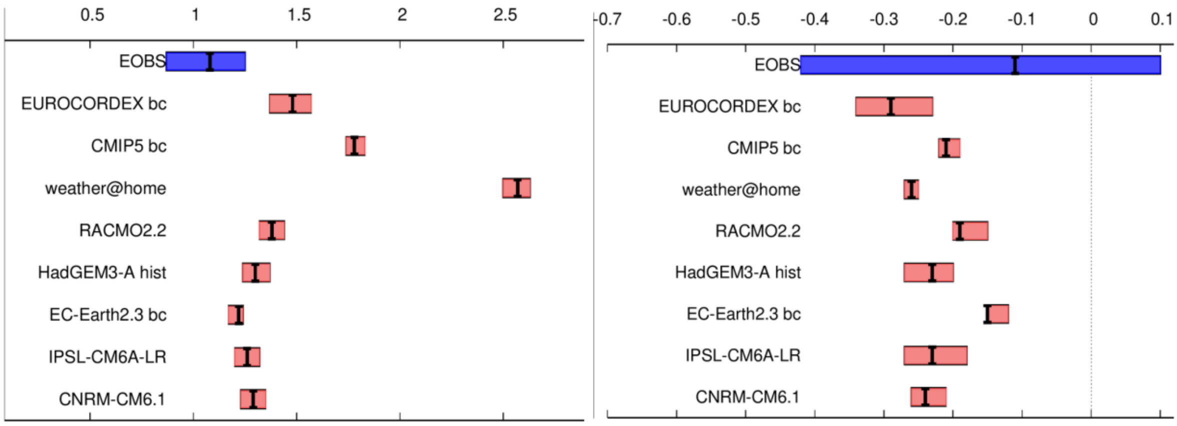

France-Average

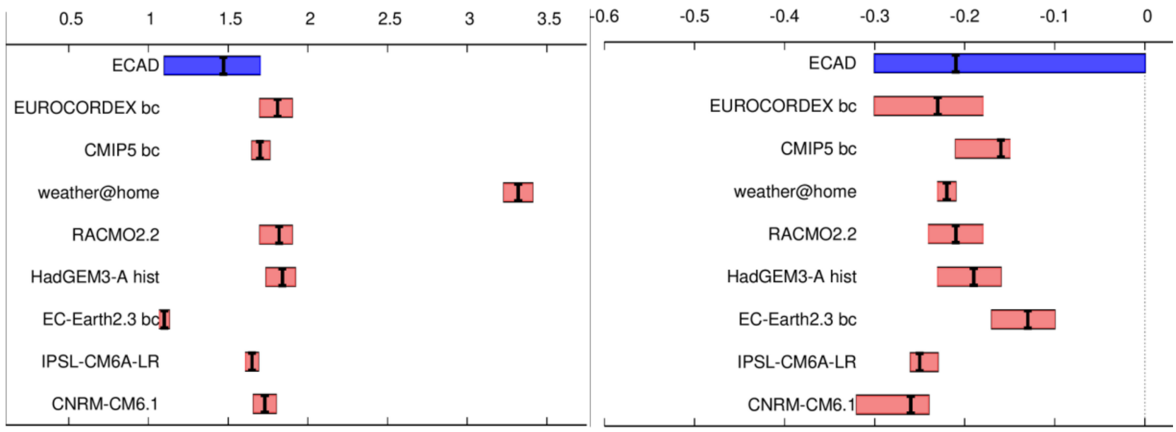

Lille-Lesquin

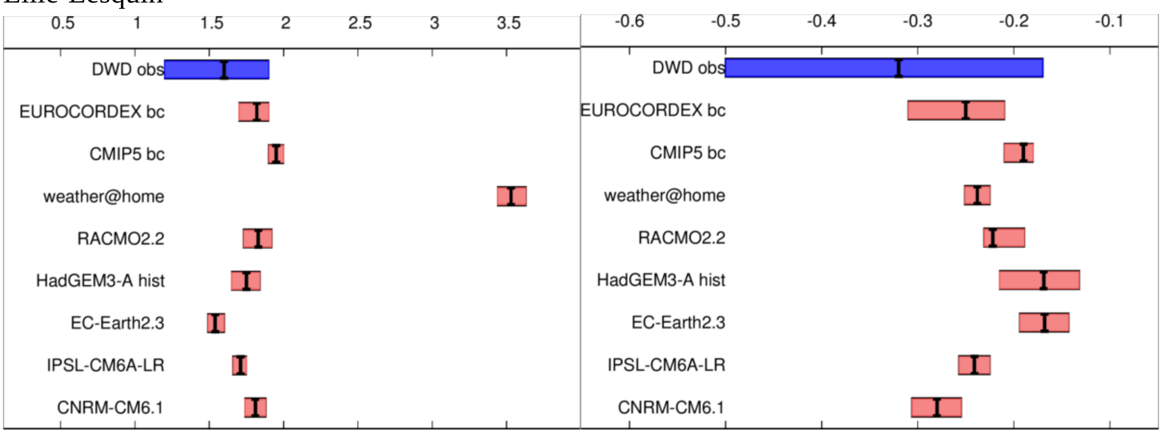

Weilerswist-Lommersum

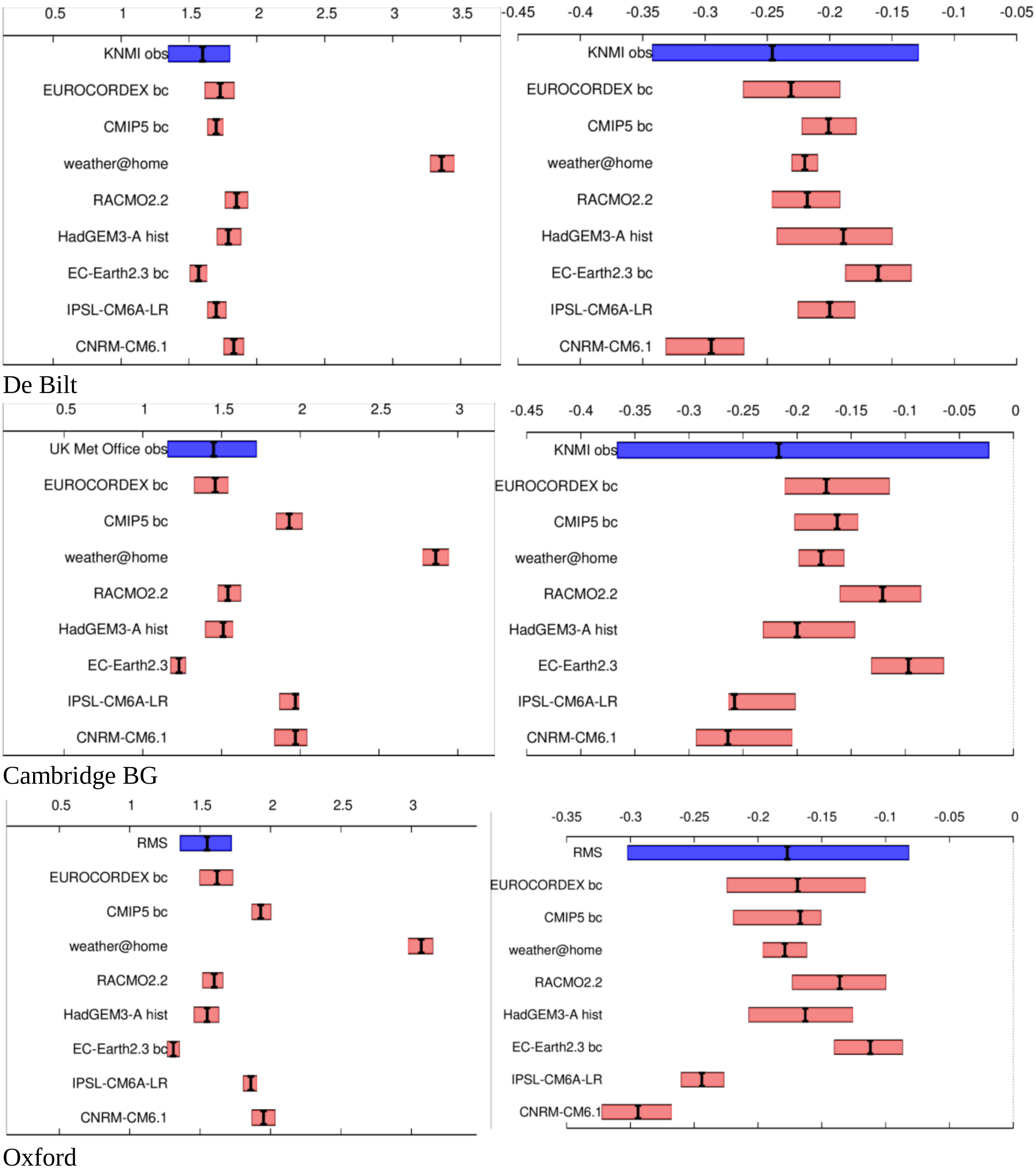

Figure 5: Estimates of the scale (left panels) and shape (right panels) parameters of the fitted GEV distribution with smooth GMST as covariate for both models and observations for each location. From top to bottom: France-Average, Lille, Weilerswist-Lommersum, De Bilt, Cambridge and Oxford. The bars denote the 95% confidence intervals estimated with a nonparametric bootstrap of 1000 samples.

Attribution

The attribution of the changes in frequency or intensity of the heat such as observed in the selected locations in Europe to human-induced climate change is carried out for each location using the subset of 8 model ensembles that passed the model evaluation tests of the previous section. We now describe results by location, grouped by country.

The attribution is carried out using estimations from a GEV fit with the smoothed GMST covariate as an indicator of climate change and human activities. The training period for the fit is taken as the largest possible period between 1900 and 2019 for models and ending in 2018 for the observations in order not to include the extreme event itself as it would lead to a selection bias. For some model ensembles the fit was made over a shorter period as the data were not available back to 1900 (such as for RACMO, EURO-CORDEX and HadGEM3-A). Due to the large ensemble size in the weather@home simulations no distribution was fitted but a non-parametric comparison of the observed event in the simulation of the present day climate with the same event in a counterfactual climate performed.

A synthesis is made based on observations and the model ensembles that passed the evaluation by weighting the results. The model results are combined with an estimate of model uncertainty such that the spread in the model results is compatible with the total uncertainty, which is the uncertainty due to natural variability combined with this model uncertainty (so we fit the model uncertainty to give $\chi^2/\mathrm{dof} = 1$). The same model uncertainty is added to the "models" subresult. This subresult is combined with the observed estimate in two ways: a weighted average denoted by the coloured bar and an unweighted average denoted by the open bar. As the models have more biases than the spread indicates we base our conclusions on the latter, which gives more weight to the observations (the method is described in detail in van Oldenborgh et al, in preparation, a copy of the draft is available on request).

France

Figure 6 shows attribution results for (i) the average over metropolitan France and (ii) the Lille station. Detailed numerical results can also be found in the Appendix.

For the France average, the heatwave was an event with a return period estimated to be 134 years. Models generally exhibit a smaller change in intensity and likelihood than the observations. Except for HadGEM-3A, which has a hot and dry bias, the changes in intensity are underestimated, as they range from 1.1°C (CNRM-CM6.1) to 1.6°C (EC-EARTH). The probability ratios are large, variable, and for HadGEM3-A could not even be estimated.

By combining information from models and observations, we conclude that the probability of such an event to occur for France has increased by a factor of at least 10 (see the synthesis in Figure 6). This factor is very uncertain and could also be two orders of magnitude higher. The change in intensity of an equally probable heatwave is between 1.5 and 3 degrees.

For Lille, results are similar. The best estimate of the return period is 78 years. The changes in intensity are similar as for France in the models, but the observation exhibits a best estimate of 3.5°C. Changes in probabilities are also extremely large, at least a factor of ~10 and a range of intensity increase of about 1.5°C to 3°C as seen from the synthesis in the Figure 6. However models predict trend estimates that are inconsistent with observation trends, a fact that needs further investigation beyond the scope of this attribution study.

We conclude that such an event would have had an extremely small probability to occur (less than about once every 1000 years) without climate change in France. Climate change had therefore a major influence to explain such temperatures, making them about 100 times more likely (at least a factor of ten).

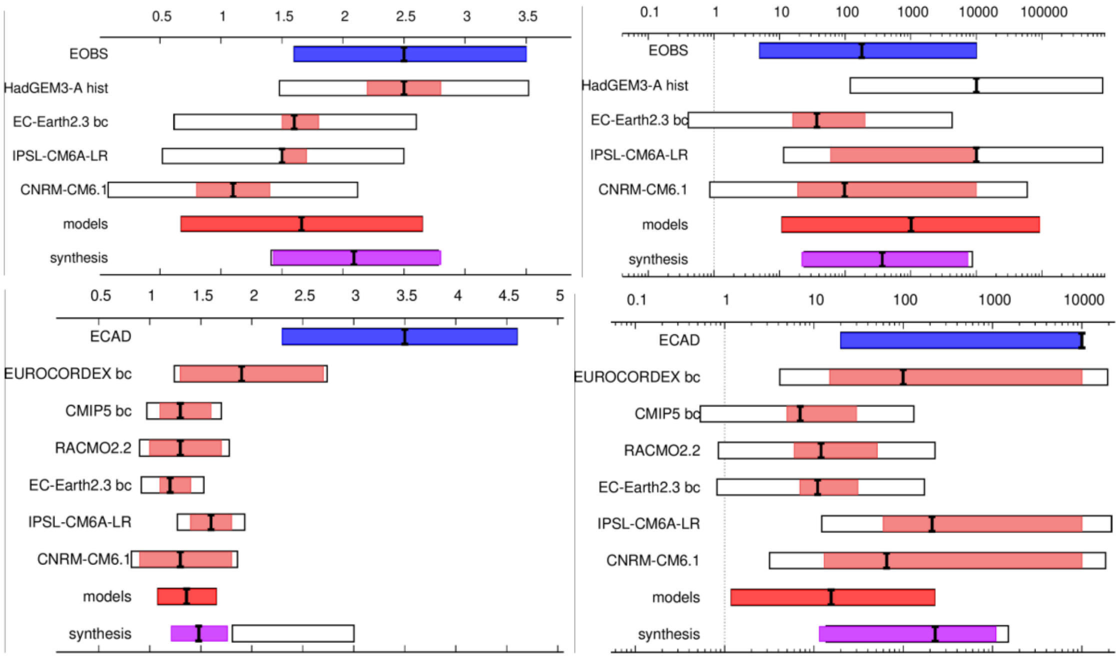

Figure 6: Changes in intensity (left panels) and probability ratios (right panels) obtained for all models and the two stations in France. From top to bottom: France Average, Lille-Lesquin.

Germany

For Germany, we analysed Weilerswist-Lommersum, which has a time series going back to 1937 with only two missing years. The changes in temperature are, as for France, largely underestimated by the models compared to observations by all but the HadGEM3-A model. Based on observations and models, we find that the effect of climate change on heatwave intensity was to elevate temperatures by 1.5 to 3.5 degrees (synthesis in Figure 7).

Because the event was less rare than in France, the probability ratios are also less extreme. Again all models except HadGEM3-A multi-model ensemble underestimate the trend up to now. This leads to (much) lower probability ratios in these models than in the observations. The combination of models and observations leads to an increase of at least a factor ~50 (at least eight).

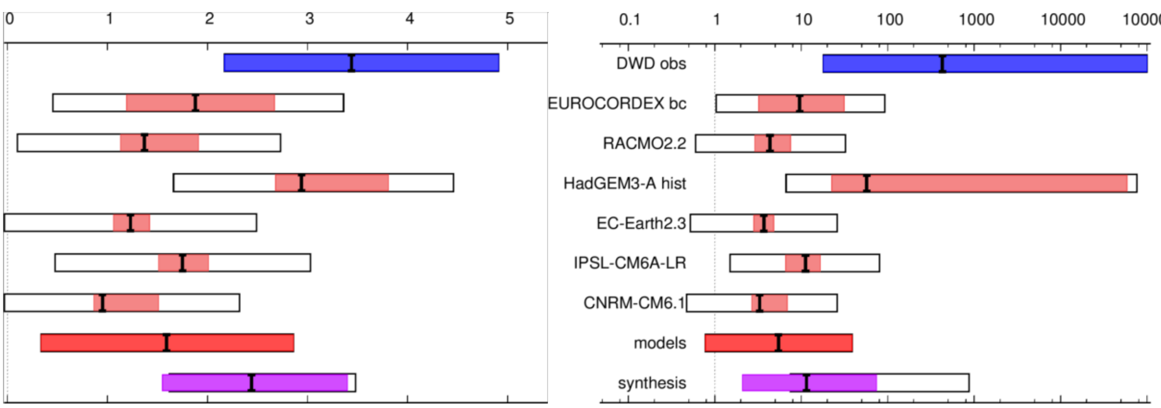

Figure 7: Changes in intensity (left panels) and probability ratios (right panels) obtained for all models and the station of Weilerswist-Lommersum

The Netherlands

The change in temperature of the hottest three days of the year is 2.9±1.0 ºC in the observations and around 1.5 ºC in all models except HadGEM3-A (which has a dry and warm bias) and EURO-CORDEX (which has no aerosol changes except for one of the models). The large deviation of HadGEM3-A from the other models gives rise to a large model spread term (white boxes, which increases the uncertainty on the model estimate so that it agrees with the observed trend). Without the HadGEM3-A the models agree well with each other but not with the observations (not shown). The overall synthesis provides, as for France, an intensity change in the range of 1.5 to 3 degrees.

For the Probability Ratio, we arbitrarily replaced the infinities by 10000 yr and 100000 yr for the upper bound on the PR of the fit to the observations. As expected the models show (much) lower PRs, due to the higher variability and lower trends. The models with the lowest trends, EC-Earth and RACMO, also give the lowest Probability Ratio, around 10. Combining models and observations gives a best estimate of 300 with a lower bound of 25.

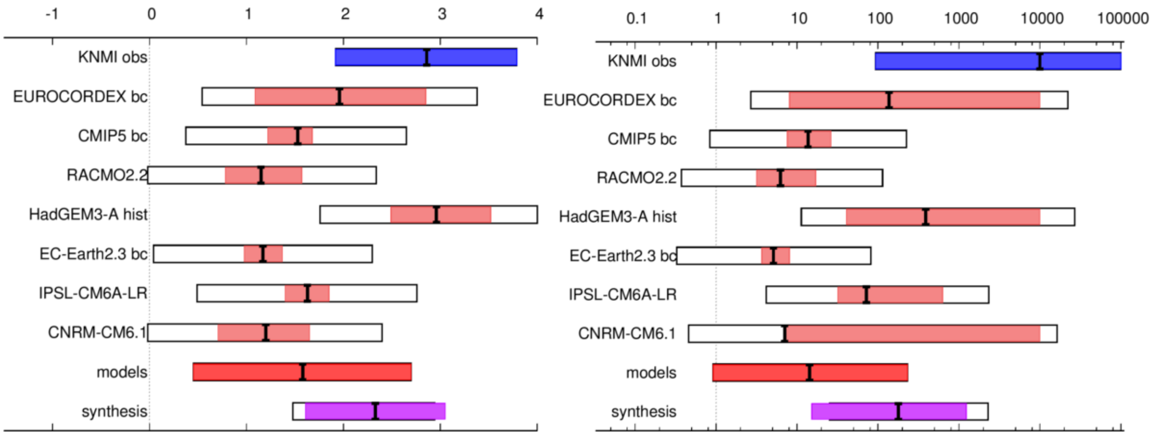

Figure 8: Changes in intensity (left panels) and probability ratios (right panels) obtained for all models at the station of De Bilt.

U. K.

For U.K. stations, only 4 (Cambridge) and 3 (Oxford) model ensembles were kept in the analysis based on our selection criteria. As for the other locations, Probability Ratios cover a wide range. Combining observations and models lead us to conclude that the likelihood of the event has increased by a factor of ~20 in Cambridge (at least a factor of 3). For Oxford on the other hand, the heatwave was less extreme in TG3x and the PR numbers are lower.

Interestingly, the change in intensity is better simulated than for other continental locations. Based on all information we find a rather similar range of temperature trends, from slightly less than 1.5 to ~2.5 degrees. The range is slightly higher for Cambridge than for Oxford.

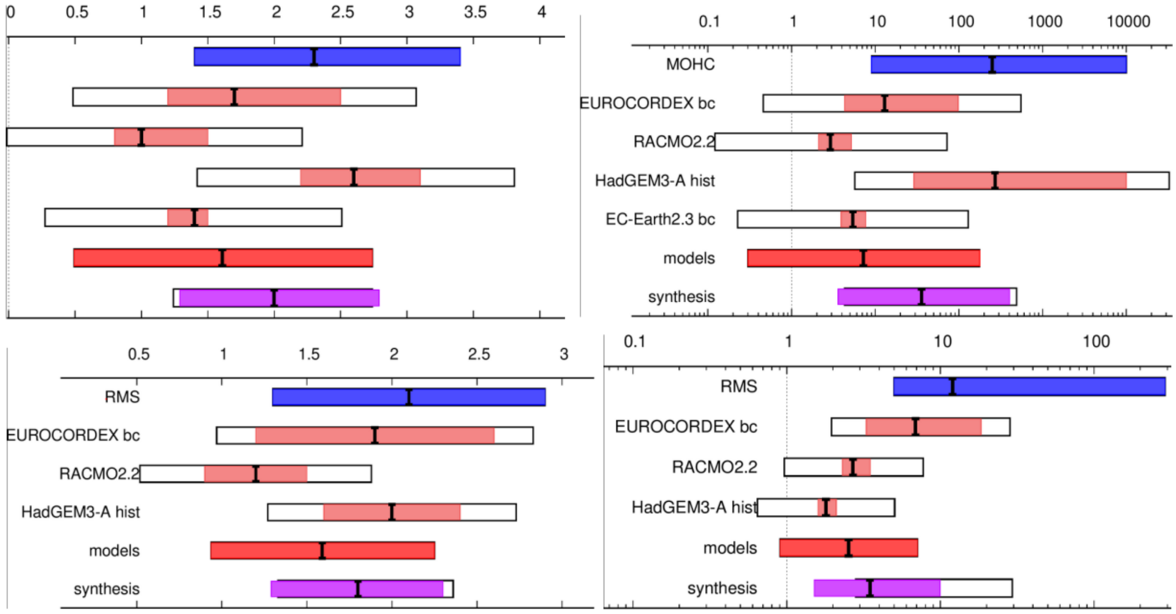

Figure 9: Changes in intensity (left panels) and probability ratios (right panels) obtained for all models and the two stations in the U.K. From top to bottom: Cambridge, Oxford.

Hazard synthesis

The heatwave that struck western Europe was rather short lived (3-4 days), yet very extreme as far as the highest temperatures are concerned (many records broken in most countries of Western Europe, including historical records exceeded by 1-2 degrees). From our analysis, the core of the heat anomaly appears to lie between France and the Netherlands where analyzed return periods are highest under current climate conditions (in the range of 50 to 150 years). However, our analysis reveals that the return periods can vary by large amounts from place to place. Despite the national U. K. historical record set on 25 July, the event was even shorter (1-2 days) and on a 3-day scale the event had a return period of only ~10 years.

Eight model ensembles, including two of the new CMIP6 models, were analysed using the same event definition (3-day average of mean daily temperature) and methodology, together with observations, for attributing the changes in both intensity and probability of the event at 6 locations in France, Germany, the Netherlands and U.K..

The models generally have too large a variability compared to observations, but the observations have a heavier tail than the models, which have too negative a shape parameter. As for the June 2019 case, models have extreme temperature trends lower than observations on the continent, with a factor up to two or more in some cases (such as for Lille and De Bilt).

Taking this into account, our analysis reveals the following robust findings:

- at all locations analyzed, the combination of observations and model results indicate that temperature trends associated to this extreme event are in the approximate range of 1.5 to 3 degrees. This indicates that without human-induced climate change a heatwave as exceptional as this one would have had temperatures about 1.5 to 3 degrees lower, temperature differences consistent with increased instances of morbidity and mortality. Baccini et al 2008

- at all locations analyzed, the change in probability of the event is large, and in several cases it is so large that a reliable estimate cannot be established. In France and the Netherlands, we find changes of at least a factor 10, meaning that the event would be extremely improbable without climate change (return period larger than about 1000 years). For the other locations, changes in probabilities were less impressive but still very large, at least a factor of 2-3 for the U.K. station, and 8 for the German station.

This analysis, together with the analysis of the June case, triggers several key research questions, which are:

- what are the physical mechanisms involved in explaining the common model biases in the extremes (eg. too high variability, too small trends)?
- would one obtain similar results using different statistical methods (only one method has been applied), and other conditionings?
- are models improving on the simulation of extremes, from the CMIP5 to CMIP6 generation?
- has climate change induced more atmospheric flows favorable to extreme heat, and, vice versa, for similar flows what are the changes in temperatures?

These yet unsolved questions call for more investigation which could not be carried out in this rapid attribution study.

Vulnerability and Exposure

Heatwaves are amongst the deadliest natural disasters facing humanity today and their frequency and intensity is on the rise globally. Consistent with this trend, the July 2019 heatwave across parts of Europe was made more likely due to climate change, as documented in this study. Combined with other risk factors such as age, certain non-communicable diseases, socio-economic disadvantages, and the urban heat island effect, extreme heat impacts become even more acute. (Kovats and Hajat 2008)

The most striking impacts of heatwaves, deaths, are not fully understood until weeks, months or even years after the initial event. While a few initial deaths due to heat stroke and drowning (from people attempting to keep cool at beaches and pools) may be reported, these numbers consistently pale in comparison to deaths resulting from excess mortality. Excess mortality is derived from statistical analysis comparing deaths during an extreme heat event to the typical projected number of deaths for the same time period based on historical record. (McGregor et al 2015) Those at highest risk of death during a heatwave are older people, people with respiratory illnesses, cardiovascular disease and other pre-existing conditions, homeless, socially isolated, urban residents and others. (McGregor et al 2015) Deaths among these populations are are not attributable to instances of extreme heat in real time but become apparent through a public health lens following the event. The 2003 European heatwave was originally estimated to have 35,000 excess deaths, this number was later estimated to be 70,000 excess deaths in 2008. (Robine et al 2008) The Russian heatwave of 2010 was estimated to have 55,000 excess deaths, due in part to a combination of extreme heat and excess air pollution. (Shaposhnikov at al 2014) A 2010 heatwave in India was estimated to have caused 1,344 excess deaths, a 43.1% increase over average, in a 2014 study. (Azhar 2014) This lag time between the occurrence of the heatwave, and an understanding of excess deaths poses significant barriers to public action to reduce heat risks. Yet, simple, low cost measures can prevent heat deaths.

Following Europe's extreme heat event of 2003 many life saving measures have been put in place. The Netherlands established a 'National Heatwave Action Plan', France established the 'Plane Canicule', in Germany a heat wave warning system has been established and The United Kingdom established 'The Heatwave Plan for England'. Collectively these plans include many proven good practices such as: understanding local thresholds where excess heat becomes deadly, establishing early warning systems, bolstering public communications about heat risks , ensuring people have access to cool spaces for a few hours a day, such as cooling centers, fountains and green spaces, and bolstering health systems to be prepared for a surge in demand. (Public Health England 2019, Fouillet et al 2008, Ebi et al 2004)

However while these strong examples exist, on a whole, Europe is still highly vulnerable to heat extremes, with approximately 42% of its population over 65 vulnerable to heat risks. (Lancet 2018) In addition to life saving measures during a heatwave, it is also crucial to catalyze longer-term efforts to adapt to raising heat risks in Europe. (Bittner et al 2014) This includes increasing urban green spaces, increasing concentrations of reflective roofs, upgrading building codes to increase passive cooling strategies, and further bolstering health systems to be prepared for excess case loads. (Singh et al 2019) The City of Paris is one of the cities in Europe leading the way on this effort. Their Paris Adaptation Strategy includes measures such as: ensuring everyone in the city is a 7-minute walk, or less, from a green space with drinking water; incorporating durable water cooling systems into the urban landscape (fountains, reflecting pools, misting systems etc.); planting 20,000 trees; establishing 100 hectares of green roofs; integrating passive cooling measures into new and existing buildings and updating building codes. (Mairie de Paris 2015) Expanding measures such as these throughout urban areas across Europe will help to reduce the vulnerability and exposure of Europe's residents to future heat extremes.

Acknowledgements:

The study was made possible thanks to a strong international collaboration between several institutes and organizations in Europe (DWD, ETHZ, IPSL, ITC/Red Cross/Red Crescent, KNMI, Météo-France, Univ. Oxford, U.K. Met Office), whose teams shared data and methods, and thanks to the Climate Explorer tool developed by KNMI. It was also supported by the EU ERA4CS "EUPHEME" research project, grant #690462.

Appendix:

model details:

EURO-CORDEX: we use here an ensemble of 10 GCM-RCM models that were also used in previous studies for heatwaves, heavy precipitation and storms (see eg. Kew et al., 2019; Luu et al., 2019; Vautard et al., 2019). These models were bias-adjusted using the CDFt method (Vrac et al., 2016) using a methodology that was deployed for serving the energy sector within the Copernicus Climate Change Service (Bartok et al., submitted to Climate Services). It uses historical simulations before 2005 and the RCP4.5 scenario after then.

List of models used for EURO-CORDEX

	Global Climate Model	Regional Climate Model (downscaling)
1	CNRM-CERFACS-CNRM-CM5	ARPEGE (stretched)
2	CNRM-CERFACS-CNRM-CM5	RCA4
3	ICHEC-EC-ECEARTH	RCA4
4	ICHEC-EC-ECEARTH	RACMO22E
5	ICHEC-EC-ECEARTH	HIRHAM5
6	IPSL-IPSL-CM5A-MR	WRF331F
7	MOHC-HadGEM-ES	RACMO22E
8	MOHC-HadGEM-ES	RCA4
9	MPI-M-MPI-ESM-LR	REMO2009
10	MPI-M-MPI-ESM-LR	RCA4

CMIP5 global climate model simulations: We use here single runs (r1i1p1) of 28 model simulations from the 5th phase of the Coupled Modeling Intercomparison Project (CMIP5; Taylor, et.al. 2012) for historical and future simulations under a high emission scenario (RCP8.5, van Vuuren et al. 2011); see Table 2) building upon previous analyses with these data (e.g. Vogel et al. 2019). We compute TG3x between 1870-2100 from daily air temperatures (*tas* in CMIP5) for each model in the original resolution and then average over metropolitan France and Toulouse. For the covariate we compute mean summer temperatures on land over Western European (35°N-72N, 15°W-20°E).
All temperatures from the CMIP5 ensemble simulations are bias corrected to E-OBS (Haylock et al. 2008) temperatures for the reference period 1950-1979 for each model individually. To fit GEVs we pool the data from the whole CMIP5 ensemble from 1947-2018 which allows a robust estimate.

Table 2. Overview of 28 CMIP5 models used in this study. For each model we use one ensemble member from the historical period and RCP8.5.

Model name	Modeling center
ACCESS1.0	Commonwealth Scientific and Industrial Research Organization (CSIRO) and Bureau of Meteorology (BOM), Australia\
ACCESS1.3	Commonwealth Scientific and Industrial Research Organization (CSIRO) and Bureau of Meteorology (BOM), Australia\\
BCC-CSM1.1	Beijing Climate Center, China Meteorological Administration

BCC-CSM1.1M	Beijing Climate Center, China Meteorological Administration
CanESM2	Canadian Centre for Climate Modelling and Analysis
CCSM4	National Center for Atmospheric Research
CESM1(BGC)	Community Earth System Model Contributors
CMCC-CESM	Centro Euro-Mediterraneo sui Cambiamenti Climatic
CMCC-CM	Centro Euro-Mediterraneo sui Cambiamenti Climatici
CMCC-CMs	Centro Euro-Mediterraneo sui Cambiamenti Climatici
CNRM-CM5	Centre National de Recherches Météorologiques / Centre Européen de Recherche et Formation Avancée en Calcul Scientifique\\
CSIRO-Mk3.6.0	Commonwealth Scientific and Industrial Research Organization in collaboration with Queensland Climate Change Centre of Excellence
EC-EARTH	European-Earth-System-Model Consortium
GFDL-CM3	NOAA Geophysical Fluid Dynamics Laboratory
HadGEM2-A0	Met Office Hadley Centre
HadGEM2-CC	Met Office Hadley Centre
INM-CM4	Institute for Numerical Mathematics
IPSL-CM5A-LR	Institut Pierre-Simon Laplace
IPSL-CM5A-MR	Institut Pierre-Simon Laplace
IPSL-CM5B-LR	Institut Pierre-Simon Laplace
MIROC-ESM	Japan Agency for Marine-Earth Science and Technology, Atmosphere and Ocean Research Institute (The University of

	Tokyo), and National Institute for Environmental Studies
MIROC-ESM-CHEM	Japan Agency for Marine-Earth Science and Technology, Atmosphere and Ocean Research Institute (The University of Tokyo), and National Institute for Environmental Studies\\
MIROC5	Atmosphere and Ocean Research Institute (The University of Tokyo), National Institute for Environmental Studies, and Japan Agency for Marine-Earth Science and Technology \\
MPI-ESM-LR	Max-Planck-Institute for Meteorology
MPI-ESM-MR	Max-Planck-Institute for Meteorology
MRI-CGCM3	Meteorological Research Institute
MRI-ESM1	Meteorological Research Institute
NorESM1-M	Norwegian Climate Centre\

RACMO 2.2: this regional climate model ensemble downscales 16 initial-condition realizations of the EC-EARTH 2.3 coupled climate model in the CMIP5 RCP8.5 scenario (Lenderink et al., 2014; Aalbers et al., 2017) on a smaller European domain over 1950-2100.

HadGEM3-A-N216: the atmosphere-only version of the Hadley Centre climate model. For the trend analysis we use the 15 members run for the EUCLEIA project 1961-2015.

EC-Earth 2.3: a coupled GCM, 16 members using historical/RCP8.5 forcing over 1861-2100 (Hazeleger et al, 2010), each producing a transient climate simulation from 1860 to 2100. The model resolution is T159 which translates to around 150 km in the European domain. The underlying scenarios are the historical CMIP5 protocols until the year 2005 and the RCP8.5 scenario (Taylor et al. 2012) from 2006 onwards. Up to about 2030, the historical and RCP8.5 temperature evolution is very similar.

RACMO is a regional climate model developed at KNMI. An ensemble of sixteen members was generated to downscale the above-mentioned EC-Earth experiments over the period 1950-2100 at a resolution of about 11km (Lenderink et al., 2014, Aalbers et al., 2017).

The 15 HadGEM3-A atmosphere-only runs from 1960–2015 (Ciavarella et al, 2017) (N216, about 60km) are evaluated for the separate regions. The model is driven by observed forcings and sea-surface temperatures (SSTs) (“historical”) and with preindustrial forcings and SSTs from which the effect of climate change has been subtracted (“historicalNat”). The latter change has been estimated from the Coupled Model Intercomparison Project phase 5 (CMIP5) ensemble of coupled climate simulations.

Weather@home: Using the distributed computing framework known as weather@home (Guillod et al., 2017, Massey et al., 2015) we simulate two different large ensembles of June and July weather, using the Met Office Hadley Centre regional climate model HadRM3P at 25km resolution over Europe embedded in the atmosphere-only global circulation model HadAM3P. The first set of ensembles represents possible weather under current climate conditions (prescribed OSTIA sea surface temperatures for 2006-2015). This ensemble is called the “all forcings” scenario and includes human-caused climate change. The second set of ensembles represents possible summer weather in a world as it might have been without anthropogenic climate drivers. This ensemble is called the “natural” or “counterfactual” scenario with prescribed sea surface temperatures obtained from CMIP5 simulations (Schaller et al., 2016).

IPSL-CM6A-LR is the latest version of the IPSL climate model which was prepared for CMIP6 (publications in preparation, Servonnat et al., 2019; Lurton et al., 2019). It couples the LMDZv6 atmospheric model, the NEMO ocean, sea ice and marine biogeochemistry model and the ORCHIDEE land surface model. The resolution of the atmospheric model is 144x143 points in longitude and latitude, which corresponds to an average resolution of 160 km, and 79 vertical layers. The resolution of the ocean model is 1°x1° and 75 layers in the vertical. An ensemble of 31 historical simulations have been run for CMIP6 for the period 1850-2014 and have been prolonged until 2029 with SSP585 radiative forcings (except for constant 2014 aerosol forcing). LMDZv6 includes a ``New Physics" package based on a full rethinking of the parametrizations of turbulence, convection and clouds on which the IPSL-CM6A-LR climate model is built.

CNRM-CM6.1 is the latest version of the CNRM climate model which was prepared for CMIP6 (Voldoire et al., 2019). It couples the ARPEGE model for the atmosphere, NEMO for the ocean, ISAB-CTRIP for land surface, GELATO for sea ice. The atmospheric horizontal resolution is about 1.4° at the equator, with 91 vertical layers. The atmospheric and land surface models have been subject to major improvements since the CMIP5 exercice, and the model exhibits a higher equilibrium climate sensitivity (4.9°C). Simulations performed in the framework of the CMIP6 exercice included 10 historical runs, extending from 1850 to 2014, and SSP585 scenarios, which were used in this analysis.

Model evaluation details

Comparison of fit parameters of the tail for France average (covariate GMST)

	scale parameter σ	shape parameter ξ	
E-OBS	1.08 *[0.87-1.25]*	-0.11 *[-0.42 - 0.10]*	Ref
EURO-CORDEX (10)	1.48 *[1.37 - 1.57]*	-0.29 *[-0.34 - -0.23]*	σ wrong
CMIP5	1.78 *[1.74 - 1.83]*	-0.21 *[-0.22 - -0.19]*	σ wrong
weather@home	2.57 [2.5 - 2.63]	-0.26 [-0.27 - -0.25]	σ wrong
RACMO2.2	1.38 *[1.32 - 1.44]*	-0.19 *[-0.20 - -0.15]*	σ wrong
HadGEM3-A trend	1.30 *[1.24 - 1.37]*	-0.23 *[-0.27 - -0.20]*	just OK
EC-Earth 2.3	1.22 *[1.17 - 1.24]*	-0.15 *[-0.15 - -0.12]*	OK
IPSL-CM6A-LR	1.26 *[1.20 - 1.32]*	-0.23 *[-0.27 - -0.18]*	just OK
CNRM-CM6.1	1.29 *[1.23 - 1.35]*	-0.24 *[-0.26 - -0.21]*	just OK

Comparison of fit parameters of the tail for Lille Lesquin Airport (covariate GMST)

	scale parameter σ	shape parameter ξ	
ECA&D	1.47 *[1.1 - 1.7]*	-0.21 *[-0.3 - 0.0]*	Ref.
EURO-CORDEX (BC)	1.81 *[1.7 - 1.9]*	-0.23 *[-0.30 - -0.18]*	just OK
CMIP5	1.70 *[1.65 - 1.76]*	-0.16 *[-0.21 - -0.15]*	OK
weather@home	3.32 *[3.23 - 3.41]*	-0.22 *[-0.23 - -0.21]*	σ wrong
RACMO2.2	1.82 *[1.7 - 1.9]*	-0.21 *[-0.24 - -0.18]*	just OK
HadGEM3-A trend	1.84 *[1.74 - 1.92]*	-0.19 *[-0.23 - -0.16]*	σ wrong
EC-Earth 2.3	1.10 *[1.07 - 1.13]*	-0.13 *[-0.17 - -0.10]*	OK
IPSL-CM6A-LR	1.65 *[1.61 - 1.69]*	-0.25 *[-0.26 - -0.23]*	OK
CNRM-CM6.1	1.73 *[1.66 - 1.80]*	-0.26 *[-0.32 - -0.24]*	OK

Comparison of fit parameters of the tail for De Bilt.

	scale parameter σ	shape parameter ξ	
KNMI homogenised	1.601 1.349... 1.801	-0.246 -0.342... -0.129	Ref.
EURO-CORDEX (10)	1.734 1.625... 1.834	-0.231 -0.269... -0.192	OK
CMIP5	1.701 1.642... 1.755	-0.201 -0.222... -0.179	OK
weather@home	3.36 [3.28 - 3.45]	-0.22 [-0.23 - -0.21]	too high

RACMO2.2	1.851 1.770... 1.934	-0.218 -0.246... -0.192	OK
HadGEM3-A trend	1.793 1.706... 1.880	-0.189 -0.242... -0.150	OK
EC-Earth 2.3 bc	1.574 1.511... 1.629	-0.161 -0.187... -0.135	bc
IPSL-CM6A-LR	1.704 1.645... 1.768	-0.200 -0.225... -0.180	OK
CNRM-CM6.1	1.830 1.757... 1.901	-0.295 -0.331... -0.269	OK

Comparison of fit parameters of the tail for Weilerswist-Lommersum.

	scale parameter σ	shape parameter ξ	
DWD	1.594 1.320... 1.816	-0.199 -0.338... -0.101	Ref
EURO-CORDEX (10)	1.791 1.648... 1.903	-0.221 -0.253... -0.160	OK
CMIP5*	1.95 *[1.9 - 2.0]*	-0.19 *[-0.21 - -0.18]*	σ wrong
weather@home	3.53362 [3.44117, 3.62855]	-0.237846 [-0.251033, -0.224659]	σ wrong
RACMO2.2	1.707 1.615... 1.799	-0.196 -0.220... -0.144	OK
HadGEM3-A trend	1.663 1.585... 1.798	-0.194 -0.265... -0.145	OK
EC-Earth 2.3	1.375 1.341... 1.455	-0.131 -0.168... -0.107	OK
IPSL-CM6A-LR*	1.705 1.664... 1.747	-0.241 -0.257... -0.225	OK
CNRM-CM6.1*	1.810 1.738... 1.879	-0.280 -0.306... -0.255	OK

*at the location of Lingen, 200 km to the north.

Comparison of fit parameters of the tail for Cambridge BG.

	scale parameter σ	shape parameter ξ	
MOHC	1.453 1.156... 1.724	-0.217 -0.366... -0.023	Ref.
EURO-CORDEX (10)	1.459 1.331... 1.544	-0.173 -0.211... -0.115	bc
CMIP5	1.931 1.854... 2.005	-0.163 -0.202... -0.144	σ wrong
weather@home	2.86218 [2.78411, 2.94244]	-0.177752 [-0.19839, -0.157115]	σ wrong
RACMO2.2	1.537 1.480... 1.618	-0.121 -0.160... -0.086	OK
HadGEM3-A trend	1.507 1.396... 1.565	-0.200 -0.231... -0.147	OK
EC-Earth 2.3	1.231 1.180... 1.273	-0.097 -0.131... -0.065	OK
IPSL-CM6A-LR	1.971 1.867... 1.992	-0.258 -0.263... -0.202	σ wrong

CNRM-CM6.1	1.967 1.842... 2.036	-0.264 -0.293... -0.205	σ wrong

Comparison of fit parameters of the tail for Oxford.

	scale parameter σ	shape parameter ξ	
RMS	1.55 1.359 1.716	-0.177 -0.302 -0.082	Ref.
EURO-CORDEX (10)	1.616 1.499 1.728	-0.169 -0.224 -0.116	bc
CMIP5	1.934 1.872 1.997	-0.167 -0.219 -0.151	bc
weather@home	3.06572 2.98365 3.15004	-0.179126 -0.195901 -0.162352	
RACMO2.2	1.595 1.524 1.657	-0.136 -0.173 -0.100	
HadGEM3-A trend	1.548 1.464 1.631	-0.163 -0.207 -0.126	
EC-Earth 2.3	1.310 1.267 1.348	-0.112 -0.140 -0.087	
IPSL-CM6A-LR	1.859 1.811 1.899	-0.244 -0.260 -0.227	
CNRM-CM6.1	1.953 1.869 2.028	-0.294 -0.322 -0.268	

Attribution details

Changes for Metropolitan France average. Grey indicates models that did not pass the model evaluation test, notably because the variability is incompatible with the observations (too high).

	ref yrs	Return Value (°C) RP=134yr	Probability Ratio	Change in temperature (°C)
E-OBS	1950-2018	**28.2**	**179** *[>5]*	**2.5** *[1.6-3.5]*
EURO-CORDEX	1971-2019	27.9	> 400	1.9 *[1.2-2.6]*
CMIP5	1900-2019	26.1	11 *[5-21]*	1.2 *[0.9-1.4]*
weather@home	counterfactual 2006-2015		7.33 (3.24 - 23.21)	1.88
RACMO2.2	1950-2019	25.2	75 [>*18*]	1.6 *[1.3-1.9]*
HadGEM3-A	1960-2015	28.0	*infinite*	2.5 *[2.2-2.8]*
EC-Earth2.3	1900-2019	25.0	37 *[16-200]*	1.6 *[1.5-1.8]*
IPSL-CM6A-LR	1900-2019	28.6	28000 *[>60]*	1.5 *[1.5-1.7]*
CNRM-CM6.1	1900-2014	28.1	98 *[>19]*	1.1 *[0.8-1.4]*

Changes for Lille-Lesquin

	ref yrs	Return Value (°C) RP=78yr	Probability Ratio	Change in temperature
ECA&D	1950-2018	**29.0**	**>20**	**3.5** *[2.3 - 4.6]*
EURO-CORDEX	1971-2019	28.2	100 [>15]	1.9 *[1.3-2.7]*
CMIP5	1900-2019	27.6	7 *[5-30]*	1.3 *[1.1-1.6]*
weather@home	counterfactual 2006-2015	non sensically high	3.5 [1.9 - 6.8]	1.4
RACMO2.2	1950-2019	26.2	12 *[6-51]*	1.3 *[1.0-1.7]*
HadGEM3-A	1960-2015	29.4	360 *[>48]*	2.7 *[2.2-3.2]*
EC-Earth2.3	1900-2019	23.0	11 *[7-31]*	1.2 *[1.1-1.4]*
IPSL-CM6A-LR	1900-2019	29.6	210 *[>60]*	1.6 *[1.4-1.8]*
CNRM-CM6.1	1900-2014	30.5	65 *[>13]*	1.3 *[0.9-1.8]*

Changes for Weilerswist-Lommersum

	ref yrs	Return Value (°C) RP=12yr	Probability Ratio	Change in temperature
DWD	1951-2018	28.7	430 18... ∞	3.4 2.2 ... 4.9
EURO-CORDEX	1971-2019	27.7	9.6 3.2 ... 31	1.9 1.2 ... 2.7
CMIP5*	1900-2019	26.9	3.7 2.8 ... 4.8	1.5 1.2 ... 1.7
weather@home	counterfactual 2006-2015			
RACMO2.2	1950-2019	24.6	4.3 2.9 ... 7.4	1.4 1.1 ... 1.9
HadGEM3-A	1960-2015	27.3	57 23 ... 59000	2.9 2.7 ... 3.8
EC-Earth2.3	1900-2019	22.9	3.7 2.9 ... 4.7	1.2 1.1 ... 1.4
IPSL-CM6A-LR*	1900-2019	28.3	11 6.5 ... 16	1.8 1.5 ... 2.0
CNRM-CM6.1*	1900-2014	27.7	3.3 2.7 ... 6.9	1.0 0.8 ... 1.5

*at the location of Lingen

Changes for De Bilt

	ref yrs	Probability Ratio	Change in temperature
KNMI (28.0)	1900 2019	∞ 66.975 ... ∞	2.856 1.994 ... 3.799
EURO-CORDEX (27.5)	1971 2019	137.03 8.0631 ... ∞	1.955 1.087 ... 2.847
CMIP5 (27.4)	1900 2019	13.683 7.5778 ... 26.321	1.528 1.220 ... 1.677
weather@home	counterfactual 2006-2015	3.57 (2.1 - 8.84)	1.66
RACMO2.2 (26.0)	1900 2019	6.2387 3.1557 ... 17.000	1.155 0.783 ... 1.565
HadGEM3-A (29.4)	1900 2019	389.16 40.716 ... ∞	2.963 2.495 ... 3.520
EC-Earth2.3 bc (26.9)	1900 2019	5.1267 3.6624 ... 8.0555	1.171 0.977 ... 1.367
IPSL-CM6A-LR (29.8)	1900 2019	72.045 31.899 ... 629.82	1.627 1.398 ... 1.846
CNRM-CM6 (29.6)	1900 2019	37.050 7.1675 ... ∞	1.197 0.708 ... 1.651

Table 13: Changes for Cambridge

	ref yrs	Return Value (°C) RP = 28yr	Probability Ratio	Change in temperature
MOHC	1951-2018	26.0	250 9 ... ∞	2.3 1.4 ... 3.4
EURO-CORDEX	1971-2019	25.0	13 4.3 ... 98	1.7 1.2 ... 2.5
CMIP5	1900-2019	25.7	3.5 2.9 ... 5.5	1.3 1.1 ... 1.6
weather@home	counterfactual vs 2006-2015	30.3	2.4 [1.7 - 3.2]	1.2
RACMO2.2	1950-2019	23.3	2.9 2.1 ... 5.2	1.0 0.8 ... 1.5
HadGEM3-A	1960-2015	26.0	270 29 ... 25000.	2.6 2.2 ... 3.1
EC-Earth2.3	1900-2019	22.6	5.4 3.9 ... 7.7	1.4 1.2 ... 1.5
IPSL-CM6A-LR	1900-2019	28.1	35 9.9 ... 50	1.9 1.5 ... 2.1
CNRM-CM6.1	1900-2014	28.8	6.4 3.2 ... 16	1.2 0.8 ... 1.7

Changes for the Oxford station

	ref yrs	Return Value (°C) RP = 7.7 yrs	Probability Ratio	Change in temperature
RMS	...-2018	**25.0**	**12** *[5-290]*	**2.1** *[1.3-2.9]*
EURO-CORDEX	1971-2019	24.5	6.9 *[3.3-18.4]*	1.9 *[1.2-2.6]*
CMIP5	1900-2019	23.9	2.7 *[2.3-3.5]*	1.3 *[1.0-1.5]*
weather@home	counterfactual 2006-2015	28.6	1.8 *[1.6 - 2.1]*	0.9
RACMO2.2	1950-2019	21.7	2.8 *[2.2-4.0]*	1.2 *[0.9-1.5]*
HadGEM3-A		23.9	8.9 *[5.6-17]*	2.0 *[1.6-2.4]*
EC-Earth2.3	1900-2019	21.2	3.9 *[3.0-4.8]*	1.3 *[1.1-1.5]*
IPSL-CM6A-LR	1900-2019	25.4	5.9 *[4.7-7.6]*	1.6 *[1.4-1.8]*
CNRM-CM6.1	1900-2019	27.7	5.0 *[3.3-8.4]*	1.4 *[1.0-1.7]*

References

Aalbers, E., Lenderink, G., van Meijgaard, E., & van den Hurk, B. (2017, April). Changing precipitation in western Europe, climate change or natural variability?. In *EGU General Assembly Conference Abstracts* (Vol. 19, p. 16050).

Azhar, G., Mavalankar, D., Amruta, N., Rajiva, A., Dutta, P., Jaiswal, A., Sheffield, P., Knowlton, K., and Hess, J., Heat-Related Mortality in India: Excess All-Cause Mortality Associated with the 2010 Ahmedabad Heat Wave. PLoS ONE 9(3): e91831. https://doi.org/10.1371/journal.pone.0091831

Baccini, M., Biggeri, A., Accetta, G., Kosatsky, T., Katsouyanni, K., Analitis, A., …& Michelozzi, P. (2008) Heat Effects on Mortality in 15 European Cities. *Epidemiology* 19(5) 711-719

Bittner, M., Matthies, E., Dalbokova, D., Menne, B., (2014) Are European countries prepared for the next big heat-wave? *European Journal of Public Health* 24(4) 615-619

Christidis, N., Mitchell, D., Stott, P. A. (2019) Anthropogenic climate change and heat effects on health. International Journal of Climatology, doi:10.1002/joc.6104.

Ciavarella, A., Christidis, N., Andrews, M., Groenendijk, M., Rostron, J., Elkington, M., ... & Stott, P. A. (2018). Upgrade of the HadGEM3-A based attribution system to high resolution and a new validation framework for probabilistic event attribution. *Weather and climate extremes*, *20*, 9-32.

Ebi, K. L., Teisberg, T. J., Kalkstein, L. S., Robinson, L., & Weiher, R. F. (2004). Heat Watch/ Warning Systems Save Lives: Estimated Costs and Benefits for Philadelphia 1995–98. Bulletin of the American Meteorological Society, 85(8), 1067-1074. doi:10.1175/bams-85-8-1067

Fouillet, A., Rey, G., Wagner, V., Laaidi, K., Empereur-Bissonnet, P., Le Tertre, A., ... & Jougla, E. (2008). Has the impact of heat waves on mortality changed in France since the European heat wave of summer 2003? A study of the 2006 heat wave. *International journal of epidemiology*, *37*(2), 309-317.

Guillod, B., Jones, R. G., Bowery, A., Haustein, K., Massey, N. R., Mitchell, D. M., ... & Wilson, S. (2017). weather@ home 2: validation of an improved global–regional climate modelling system. *Geoscientific Model Development*, *10*(5), 1849-1872.

Haylock, M. R., Hofstra, N., Klein Tank, A. M. G., Klok, E. J., Jones, P. D., and New, M. (2008) A European daily high-resolution gridded data set of surface temperature and precipitation for 1950–2006, J. Geophys. Res., 113, D20119, https://doi.org/10.1029/2008JD010201.

Hazeleger, W., Severijns, C., Semmler, T., Ştefănescu, S., Yang, S., Wang, X., ... & Bougeault, P. (2010). EC-Earth: a seamless earth-system prediction approach in action. *Bulletin of the American Meteorological Society*, *91*(10), 1357-1364.

Kew, S. et al, (2019) The exceptional summer heatwave in Southern {Europe} 2017. Bull. Amer. Met. Soc., 100, S2-S5. doi:10.1175/BAMS-D-18-0109.1

Kovats, S. and Hajat, S. (2008) Heat Stress and Public Health: A Critical Review. *Annual Review Public Health* 29, 41-55 doi: 10.1146/annurev.publhealth.29.020907.090843

Lenderink, G., Van den Hurk, B. J. J. M., Tank, A. K., Van Oldenborgh, G. J., Van Meijgaard, E., De Vries, H., & Beersma, J. J. (2014). Preparing local climate change scenarios for the Netherlands using resampling of climate model output. *Environmental Research Letters*, *9*(11), 115008.

Luu, L., R. Vautard, P. Yiou, G. J. van Oldenborgh, and G. Lenderink, 2018, Attribution of extreme rainfall events in the South of France using EURO-CORDEX simulations. Geophys. Res. Lett., doi :10.1029/2018GL077807.

Mairie de Paris (2015) *Adaptation Strategy: Paris Climate & Energy Action Plan* Available at: https://api-site.paris.fr/images/76271

Massey, N., Jones, R., Otto, F. E. L., Aina, T., Wilson, S., Murphy, J. M., ... & Allen, M. R. (2015). weather@ home—development and validation of a very large ensemble modelling system for probabilistic event attribution. *Quarterly Journal of the Royal Meteorological Society*, *141*(690), 1528-1545.

McGregor, G. R., Bessemoulin, R., Ebi, K., & Menne, B. (Eds.). (2015). Heatwaves and health: Guidance on warning-system development (Vol. 1142). Geneva, Switzerland, World Meteorological Organization and World Health Organisation. Retrieved from: http://bit.ly/2NbDx4S

Murray, V., & Ebi, K. L. (2012). IPCC special report on managing the risks of extreme events and disasters to advance climate change adaptation (SREX).

Otto, F.E.L., van der Wiel, K., van Oldenborgh, G.J., Philip, S., Kew, S.F., Uhe, P. and Cullen, H. (2017) Climate change increases the probability of heavy rains in Northern England/Southern Scotland like those of storm Desmond - a real-time event attribution revisited. *Environmental Research Letters*.

Philip, S., Kew, S.F., van Oldenborgh, G.J., Aalbers, E., Vautard, R., Otto, F., Haustein, K., Habets, F. and Singh, R. (2018) Validation of a Rapid Attribution of the May/June 2016 Flood-Inducing, Precipitation in France to Climate Change. *Journal of Hydrometeorology*, 19: 1881-1898.

Public Health England (2019). Heatwave plan for England. London, UK, Crown copyright http://bit.ly/31XMamQ

Robine, J., Cheung, S., Le Roy, S., Van Oyen, H. Griffiths, C., Michel, JP., Hermann, FR., (2008) Death toll exceeds 70,000 in Europe during the summer of 2003. *Comptes Rendus Biologies* 331(2) 171-8 doi: 10.1016/j.crvi.2007.12.001

Schaller, N., A. L. Kay, R. Lamb, N. R. Massey, G.-J. van Oldenborgh, F. E. L. Otto, S. N. Sparrow, R. Vautard, P. Yiou, A. Bowery, S. M. Crooks, C. Huntingford, W. Ingram, R. Jones, T. Legg, J. Miller, J. Skeggs, D. Wallom, S. Wilson & M. R. Allen, 2015, Human influence on climate in the 2014 Southern England winter floods and their impacts. Nature climate change, doi:10.1038/nclimate2927.

Seneviratne S.I., T. Corti, E.L. Davin, M. Hirschi, E.B. Jaeger, I. Lehner, B. Orlowsky and A.J. Teuling (2010) Investigating soil moisture-climate interactions in a changing climate: A review. Earth Sci. Rev., 99,125–161.

Singh, R., Arrighi, J., Jjemba, E., Strachan, K., Spires, M., Kadihasanoglu, A., (2019) *Heatwave Guide for Cities*. Red Cross Red Crescent Climate Centre.

Stott PA, Stone DA, Allen MR. (2004) Human contribution to the European heatwave of 2003, Nature, 432, 7017, 610-614, DOI:10.1038/nature03089.

Taylor, K. E., R. J. Stouffer, and G. A. Meehl (2012) An overview of CMIP5 and the experiment design, Bull. Am. Meteorol. Soc., 93(4), 485–498.

van Vuuren, D.P., Edmonds, J., Kainuma, M. et al. Climatic Change (2011) 109, 5. https://doi.org/10.1007/s10584-011-0148-z

Vautard, R., van Oldenborgh, G.-J., Otto, F. E. L., Yiou, P., de Vries, H., van Meijgaard, E., Stepek, A., Soubeyroux, J.-M., Philip, S., Kew, S. F., Costella, C., Singh, R., and C. Tebaldi, 2019: Human influence on European wind storms such as those of January 2018. *Earth System Dynamics*, 10, 271-286.

Vogel M.M., J. Zscheischler, R. Wartenburger, D. Dee, and S.I. Seneviratne (2019, accepted). Concurrent 2018 hot extremes across Northern Hemisphere due to human-induced climate change. Earth's Future 7, https://doi.org/10.1029/2019EF001189.

Vrac, M., Noël, T. and R. Vautard, 2016: Bias correction of precipitation through Singularity Stochastic Removal: Because occurrences matter, J. Geophys. Res., 121(10), 5237-5258.